

USING BAND SUBSET SELECTION FOR DIMENSIONALITY REDUCTION IN SUPERPIXEL SEGMENTATION OF HYPERSPECTRAL IMAGERY

Mohammed Q. Alkhatib¹ and Miguel Velez-Reyes², Senior Member

¹ Abu Dhabi Polytechnic, Abu Dhabi, UAE, P.O. Box 111499

² Electrical and Computer Engineering, University of Texas at El Paso, El Paso, TX, USA, 79968
mqalkhatib@ieee.org, m.velez@ieee.org

ABSTRACT

This paper explores the use of unsupervised band subset selection (BSS) methods as a dimensionality reduction pre-processing stage in SLIC superpixel segmentation (BSS-SLIC). Several methods for column subset selection (CSS) are used for unsupervised band subset selection and the performance of the corresponding BSS-SLIC combination is studied. CSS is the problem of selecting the most independent columns of a matrix. BSS-SLIC superpixel segmentation results are evaluated in terms of the homogeneity of the resulting superpixels. Numerical experiments with HYDICE Urban and ROSIS Pavia data sets are used to study the performance of different BSS-SLIC algorithms. The quality of the resulting segmentation is evaluated by looking at the fraction of the total number of superpixels that are homogeneous. BSS-SLIC results in the higher percentage of homogeneous superpixels when compared with SLIC using all bands.

Index Terms— Band Subset Selection; Superpixel segmentation; SLIC Segmentation; Column subset selection; Dimensionality reduction.

1. INTRODUCTION

Superpixel oversegmentation breaks the image into locally homogeneous regions that are not necessarily distributed in a uniform grid. Each region could be treated as a single entity during further processing. Since the number of superpixels is in general much smaller than the number of image pixels, it can result in significant computational savings. The value of the superpixel representation in image processing and computer vision has been recognized in the literature [1].

The Simple Linear Iterative Clustering (SLIC) [2] algorithm has shown better performance in superpixel segmentation than other methods in terms of computation speed and memory efficiency. SLIC is commonly used for deriving superpixel-based representations of hyperspectral images. In many applications, the image representation is derived by representing the spectral signatures in a superpixel by their mean. The quality of this representation will depend on the homogeneity of the superpixels. Homogeneous superpixels

are well represented by their mean while non-homogeneous ones are not [3, 4].

SLIC is basically a k-means clustering algorithm with spatial adjacency constraints. We use the SLIC algorithm for hyperspectral imagery described in [5] and the MATLABTM implementation toolbox provided in [6]. The work in [5] extends the standard SLIC for color images to hyperspectral images by using the full spectral signature vector and not a three-color vector as in RGB images.

1.1. Band subset selection

Hyperspectral imagers collect hundreds of spectral images at closely spaced narrow spectral bands. The large dimensionality of these sets can present a challenge in computational requirements for hyperspectral image exploitation. Band subset selection (BSS) is a technique for dimensionality reduction (DR) that keeps spectral insight for further image exploitation. BSS can be based on physical insight, optimizing an information content measure, class separability, or other criteria. Supervised and unsupervised methods for BSS are proposed in the literature, see for examples [7, 8, 9, 10].

In hyperspectral image analysis, it is common to unfold the hyperspectral data cube into a matrix with columns representing individual bands and rows the spectral signatures of individual pixels. Therefore, BSS is related to the selection of a subset of columns from the resulting matrix.

In linear algebra, the column subset selection (CSS) is the problem of selecting the most linearly independent or most representative subset of columns of a matrix. Choosing the optimal subset is an NP-hard problem [11]. Deterministic and randomized algorithms have been proposed for CSS [12]. CSS has been explored in [7, 10, 13] for unsupervised BSS.

In this paper, we investigate the use of BSS as a pre-processing stage in SLIC superpixel segmentation. Our hypothesis is that BSS dimensionality reduction can lead to a better superpixel representation (i.e. more homogeneous superpixels) than using all the image bands.

Section 2 presents the mathematical formulation of the BSS used in this paper. Section 3 presents the CC problem and the algorithms used in this paper. Section 4 presents the

experimental methodology used and results are shown in section 5. Section 6 presents conclusions and final remarks.

2. BSS AND DIMENSIONALITY REDUCTION

BSS has several interesting advantages compared to other dimensionality reduction techniques since it preserves the physical meaning of the spectral bands that can be used to (a) maximize human understanding, (b) combine spectral data with other data types, and (c) exploit physical modeling/simulation.

In terms of the matrix representation of the hyperspectral image $\mathbf{X} \in R^{N \times n}$, BSS can be stated as the problem of selecting a permutation matrix $\mathbf{\Pi}$ in

$$\mathbf{X}\mathbf{\Pi} = [\mathbf{X}_1 | \mathbf{X}_2] \quad (1)$$

such that $\mathbf{X}_1 \in R^{N \times p}$, the matrix of "selected bands", has some particular properties of interest. $\mathbf{X}_2 \in R^{N \times (n-p)}$ is the matrix of "redundant bands". Here N is the number of pixels, and n is the number of spectral bands. Clearly, this formulation helps to relate BSS to CSS [13][14]

3. COLUMN SUBSET SELECTION PROBLEM

Given a matrix $\mathbf{X} \in R^{N \times n}$ with $N > n$, CSS can be formulated as the as the following optimization problem [11]:

$$\mathbf{\Pi}^* = \underset{\text{Subject to } \mathbf{X}\mathbf{\Pi}=[\mathbf{X}_1|\mathbf{X}_2]}{\operatorname{argmin}} \|\mathbf{X}_2 - \mathbf{X}_1 \mathbf{X}_1^\# \mathbf{X}_2\|_F^2 \quad (2)$$

The optimal $\mathbf{\Pi}$ chooses the columns that best predict the redundant columns with minimal residual error. $\mathbf{X}^\#$ is the psuedo-inverse of matrix \mathbf{X} , $\mathbf{X}_1 \in R^{N \times p}$ is commonly called the matrix of "representative columns." This is a NP-hard problem [11] for which many algorithms are proposed in the linear algebra literature that obtain good solutions.

3.1. CSS Algorithms

This section briefly describes the CSS algorithms used in this paper for unsupervised BSS.

3.1.1. SVDSS

This algorithm for CSS was proposed in [15]. Let $\mathbf{X} = \mathbf{U}\mathbf{\Sigma}\mathbf{V}^T$ be the SVD for \mathbf{X} . Note that

$$\mathbf{X}\mathbf{\Pi} = [\mathbf{X}_1 | \mathbf{X}_2] = \mathbf{U}\mathbf{\Sigma}\mathbf{V}^T \mathbf{\Pi} \quad (3)$$

Therefore, permuting the columns of \mathbf{X} is equivalent to permuting the rows of \mathbf{V} . Moreover, selecting the particular column from \mathbf{X} amounts to selecting the corresponding row in \mathbf{V} . Let

$$\bar{\mathbf{V}} = \mathbf{\Pi}^T \mathbf{V} = \begin{bmatrix} \bar{\mathbf{V}}_{11} & \bar{\mathbf{V}}_{12} \\ \bar{\mathbf{V}}_{21} & \bar{\mathbf{V}}_{22} \end{bmatrix}$$

be a partitioning of the row wise permuted matrix of right singular vectors commensurate with the partitioning in (1). It is shown in [14, 15] that a good $\mathbf{\Pi}$ is one that results in $\|\bar{\mathbf{V}}_{11}^{-1}\| \approx 1$, which can be obtained from the QR factorization with pivoting [14, 15] on the matrix \mathbf{V}_1^T corresponding to the first p right singular vectors of \mathbf{X} .

3.1.2. Rank-revealing QR factorizations

The QR factorization can also be used for CSS [16]. The QR factorization of \mathbf{X} with column pivoting is given by

$$\mathbf{X}\mathbf{\Pi} = [\mathbf{X}_1 | \mathbf{X}_2] = \mathbf{Q}\mathbf{R} = [\mathbf{Q}_1 \ \mathbf{Q}_2] \begin{bmatrix} \mathbf{R}_{11} & \mathbf{R}_{12} \\ \mathbf{0} & \mathbf{R}_{22} \end{bmatrix} \quad (4)$$

A couple of important observations are that \mathbf{X} and \mathbf{R} have the same singular values, and that

$$\mathbf{X}_1 = \mathbf{Q}_1 \mathbf{R}_{11}, \mathbf{X}_2 = [\mathbf{Q}_1 \ \mathbf{Q}_2] \begin{bmatrix} \mathbf{R}_{12} \\ \mathbf{R}_{22} \end{bmatrix}$$

Furthermore,

$$\|\mathbf{X}_2 - \mathbf{X}_1 \mathbf{X}_1^\# \mathbf{X}_2\|_F^2 = \|\mathbf{R}_{21}\|_F^2$$

Therefore, (2) can be reformulated as the problem of computing a QR factorization with pivoting that results in a small \mathbf{R}_{21} . This specific type of QR factorization is called a Rank Revealing QR (RRQR) factorization [17]. Two of these factorizations are used here. The Pivoted QR [14, 15] available in MATLAB and RRQR from [17].

4. METHODOLOGY

The goal of this work is to study the effect of BSS as a pre-processing stage for SLIC segmentation. To compare different results, the quality of the resulting SLIC segmentation is evaluated by looking at the homogeneity of the resulting superpixels as proposed in [3].

First, different CSS methods are applied to the full hyperspectral image to obtain a subset of bands for the image. In the experiment, the number of selected bands is varied between 3 to 10. The SLIC segmentation algorithm of [2] is applied to the low dimensional image. The SLIC region size is fixed to 10 based on the results of [3]. The homogeneity and heterogeneity of the resulting superpixel (SP) segmentation is evaluated.

4.1. Superpixel Homogeneity

After performing the SP segmentation, not all superpixels in the image correspond to homogeneous regions [3]. We use matrix based techniques to study superpixel homogeneity as in [4]. If we unfold the SP spectral signatures into a matrix, a homogeneous superpixel will correspond to a nearly rank-1 matrix. A heterogeneous superpixel will correspond to a higher rank matrix.

We will use the following criterion to determine the rank of the matrix that contains the spectral signatures in a superpixel [18]:

$$\hat{d} = \min \left\{ d : \frac{\sum_{i=1}^d \sigma_i^2(\mathbf{X}_{\text{SP}})}{\sum_{i=1}^r \sigma_i^2(\mathbf{X}_{\text{SP}})} \geq \tau \right\} \quad (5)$$

where \mathbf{X}_{SP} is the matrix of spectral signatures in the superpixel, $\sigma_i(\mathbf{X}_{\text{SP}})$ is the i_{th} singular value of \mathbf{X}_{SP} , r is the number of non-zero singular values of \mathbf{X}_{SP} , τ is a threshold, and \hat{d} is the estimate of the rank of the subspace that contains the spectral signatures in the superpixel. The quantity inside the brackets is usually called the percentage of the total energy explained by the first singular vectors. The threshold τ is set to 0.95 (or 95% of the total energy). This idea was proposed in [4] to study SP homogeneity.

5. EXPERIMENTS

5.1. Hyperspectral Data

5.1.1. Urban Image

HYDICE Urban scene was recorded by the HYDICE (Hyperspectral Digital Image Collection Experiment) sensor in October 1995. The scene is an urban area at Copperas Cove, Texas, USA [19]. The image is a 307 x 307 pixels scene at 2 m resolution, with 210 bands ranging from 400 nm to 2500 nm at 10 nm resolution. Channels 1–4, 76, 87, 101–111, 136–153 and 198–210 are removed (due to dense water vapor and atmospheric effects) leaving 162 bands used in the analysis. Fig. 1(a) shows a true color RGB composite of the scene.

5.1.2. Pavia University

This is a scene acquired with the ROSIS sensor during a flight campaign over Pavia, northern Italy [20]. The image consists of 103 spectral bands from 430 to 860 nm with a spectral resolution of 4 nm and a spatial resolution of 1.3 meters. Pavia University is 610 x 340 pixels. All 103 bands were considered in the analysis. Fig. 1(b) shows a true color RGB composite of the scene.

5.2. CSS Results

In the experiments, the CSS algorithms described in Subsection 3.1 are used to perform BSS for the image. the number of bands selected for each method is varied from 3 to 10.

5.3. Superpixel Segmentation

SLIC superpixel segmentation is performed on the image with region size equals to 10. This size is chosen based on the results of [3]. Superpixel homogeneity is determined using (5).

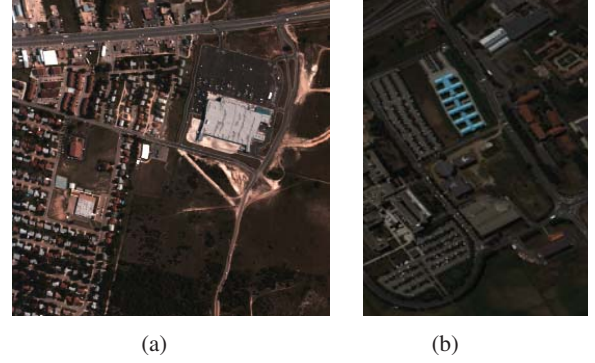


Fig. 1: True color RGB composites of (a) HYDICE Urban and (b) ROSSIS Pavia images.

Urban Image Results

Tables 1 to 3 show the resulting percentages of homogeneous superpixels for each band subset combination obtained with different CSS algorithms applied on the Urban image as the number of bands is varied from 3 to 10. It's clear that the values of the percentages varies by varying the subset of bands. The highest homogeneity percentage is highlighted in bold.

Table 4 shows summarizes the percentages obtained using all CSS algorithms mentioned in Subsection 3.1. For the SLIC region size 10, the highest percentage of homogeneous superpixels is 95.42%, obtained using the QR factorization with pivoting for 6 bands. This is higher than 89.28%, which was the percentage of homogeneous pixels obtained by using SLIC with all the bands as reported in [3].

Table 1: Results of SVDSS Algorithm [13] on Urban Image.

No. of bands	Bands	Percentage (%)
3	[63,1,134]	86.99
4	[58,93,133,14]	90.74
5	[47,58,2,93,162]	88.35
6	[95,50,58,1,94,159]	88.45
7	[83,156,70,52,123,109,2]	90.11
8	[82,84,156,49,70,123,2,109]	90.63
9	[82,84,81,156,58,49,112,128,2]	92.30
10	[82,84,162,81,156,58,49,109,132,2]	90.01

Table 2: Results of RRQR algorithm [17] on Urban Image.

No. of bands	Bands	Percentage (%)
3	[92,133,2]	88.97
4	[92,133,2,58]	91.26
5	[92,133,2,58,51]	90.53
6	[92,133,2,58,51,156]	88.76
7	[92,133,2,58,51,156,113]	89.07
8	[92,133,2,58,51,156,113,95]	89.28
9	[92,133,2,58,51,156,113,95,82]	90.32
10	[92,133,2,58,51,156,113,95,82,70]	90.84

Table 3: Results of MATLAB QR Algorithm [14, 15] on Urban Image.

No. of bands	Bands	Percentage (%)
3	[80,133,2]	87.83
4	[80,133,2,109]	90.01
5	[80,133,2,109,82]	90.84
6	[80,133,2,109,82,84]	95.42
7	[80,133,2,109,82,84,50]	92.20
8	[80,133,2,109,82,84,50,157]	90.32
9	[80,133,2,109,82,84,50,157,58]	92.20
10	[80,133,2,109,82,84,50,157,58,162]	89.80

Table 4: Summary of all percentages for different number of bands and methods for the Urban data set.

No. of bands	Urban		
	SVDSS	RRQR	QR
3	86.99	88.97	87.83
4	90.74	91.26	90.01
5	88.35	90.53	90.84
6	88.45	88.76	95.42
7	90.11	89.07	92.20
8	90.63	89.28	90.32
9	92.30	90.32	92.20
10	90.01	90.84	89.80

Pavia Results

Tables 5 to 7 show the resulting percentages of homogeneous superpixels for each band subset combination obtained by CSS applied on the Pavia University image.

Table 8 shows a summary of all percentages of homogeneous pixels obtained using all CSS algorithms mentioned in Subsection 3.1. For SLIC with region size 10, the highest percentage of homogeneous superpixels is 89.87%, obtained using the RRQR factorization with 3 bands. This is slightly higher than the one obtained by using all bands of 86.69% reported in [3]. The above results indicate that BSS may

Table 5: Results of SVDSS Algorithm [13] on Pavia Image.

No. of bands	Bands	Percentage (%)
3	[63,91,16]	89.72
4	[2,64,91,28]	87.60
5	[2,103,80,64,27]	89.34
6	[1,72,103,81,58,26]	89.68
7	[1,103,72,5,81,30,57]	88.95
8	[1,3,103,72,82,14,32,58]	87.56
9	[1,3,103,6,73,82,64,46,28]	87.41
10	[1,3,5,103,73,64,83,46,31,14]	86.74

produce a SLIC segmentation with higher number of homogeneous superpixels.

6. CONCLUSION AND FINAL REMARKS

In this paper, we compared several CSS algorithms for use in BSS dimensionality reduction in SLIC superpixel segmenta-

Table 6: Results of RRQR algorithm [17] on Pavia Image.

No. of bands	Bands	Percentage (%)
3	[91,62,16]	89.87
4	[91,62,16,34]	89.73
5	[91,62,16,34,1]	85.67
6	[91,62,16,34,1,74]	87.27
7	[91,62,16,34,1,74,3]	85.87
8	[91,62,16,34,1,74,3,103]	88.62
9	[91,62,16,34,1,74,3,103,47]	88.37
10	[91,62,16,34,1,74,3,103,47,5]	87.07

Table 7: Results of MATLAB QR Algorithm [14, 15] on Pavia Image.

No. of bands	Bands	Percentage (%)
3	[91,63,15]	89.73
4	[91,63,15,1]	85.77
5	[91,63,15,1,3]	84.71
6	[91,63,15,1,3,73]	86.01
7	[91,63,15,1,3,73,103]	89.10
8	[91,63,15,1,3,73,103,5]	88.42
9	[91,63,15,1,3,73,103,5,34]	87.60
10	[91,63,15,1,3,73,103,5,34,2]	86.93

Table 8: Summary of all percentages for different number of bands and methods for the Pavia data set.

No. of bands	Pavia		
	SVDSS	RRQR	QR
3	89.72	89.87	89.73
4	87.60	89.73	85.77
5	89.34	85.67	84.71
6	89.68	87.27	86.01
7	88.95	85.87	89.10
8	87.56	88.62	88.42
9	87.41	88.37	87.60
10	86.74	87.07	86.93

tion. Overall, the algorithms has instances that outperformed SLIC using all bands.

Table 4 shows that the QR factorization with six bands produced the highest percentage of homogeneous superpixels (95.42%) for the Urban image. For the Pavia image, Table 8 shows that CSS using the RRQR algorithm with three bands produced the highest percentage of homogeneous pixels (89.87%). These values are also higher than the ones obtained from applying SLIC using all bands (89.28% for Urban and 86.69% for Pavia) which illustrates the potential of BSS-SLIC.

Future work should consider the effect on follow-up image processing operations like unmixing or classification. That would further help to evaluate the value of BSS-SLIC. We should also look at other unsupervised BSS for this task.

7. REFERENCES

- [1] O. Lézoray, C. Meurie, and M. E. Celebi, “Special section guest editorial: Superpixels for image processing and computer vision,” *Journal of Electronic Imaging*, vol. 26, no. 06, p. 1, oct 2017.
- [2] R. Achanta, A. Shaji, K. Smith, A. Lucchi, P. Fua, and S. Süsstrunk, “SLIC superpixels compared to state-of-the-art superpixel methods,” *IEEE Transactions on Pattern Analysis and Machine Intelligence*, vol. 34, no. 11, pp. 2274–2282, 2012.
- [3] M. Q. Alkhatib and M. Velez-Reyes, “Effects of region size on superpixel-based unmixing,” in *Proceedings of the 10th Workshop on Hyperspectral Imaging and Signal Processing: Evolution in Remote Sensing (WHISPERS)*. IEEE, 2019, pp. 1–5.
- [4] J. Yi and M. Velez-Reyes, “Low-dimensional enhanced superpixel representation with homogeneity testing for unmixing of hyperspectral imagery,” in *Proceedings of SPIE*, vol. 10644, 2018, p. 1064422.
- [5] X. Zhang, S. E. Chew, Z. Xu, and N. D. Cahill, “SLIC superpixels for efficient graph-based dimensionality reduction of hyperspectral imagery,” in *Proceedings of SPIE*, vol. 9472, 2015, p. 947209.
- [6] A. Vedaldi and B. Fulkerson, “Vlfeat: An open and portable library of computer vision algorithms,” in *Proceedings of the 18th ACM International Conference on Multimedia*, ser. MM ’10. ACM, 2010, pp. 1469–1472.
- [7] C. Wang, M. Gong, M. Zhang, and Y. Chan, “Unsupervised hyperspectral image band selection via column subset selection,” *IEEE Geoscience and Remote Sensing Letters*, vol. 12, no. 7, pp. 1411–1415, 2015.
- [8] C.-I. Chang, S. Wang, K.-H. Liu, M.-L. Chang, and C. Lin, “Progressive band dimensionality expansion and reduction via band prioritization for hyperspectral imagery,” *IEEE Journal of Selected Topics in Applied Earth Observations and Remote Sensing*, vol. 4, no. 3, pp. 591–614, 2010.
- [9] S. A. Medjahed, T. A. Saadi, A. Benyettou, and M. Ouali, “Gray wolf optimizer for hyperspectral band selection,” *Applied Soft Computing*, vol. 40, pp. 178–186, 2016.
- [10] M. Velez-Reyes, D. M. Linares, and L. O. Jimenez-Rodriguez, “Two-stage band selection algorithm for hyperspectral imagery,” in *Proceedings of SPIE*, vol. 4725, 2002, pp. 30–37.
- [11] A. Çivril, “Column subset selection problem is ughard,” *Journal of Computer and System Sciences*, vol. 80, no. 4, pp. 849–859, 2014.
- [12] M. E. Broadbent, M. Brown, K. Penner, I. Ipsen, and R. Rehman, “Subset selection algorithms: Randomized vs. deterministic,” *SIAM undergraduate research online*, vol. 3, pp. 50–71, 2010.
- [13] M. Velez-Reyes and L. O. Jimenez, “Subset selection analysis for the reduction of hyperspectral imagery,” in *Proceeding of the 1998 IEEE International Geoscience and Remote Sensing. Symposium Proceedings (IGARSS)*, vol. 3. IEEE, 1998, pp. 1577–1581.
- [14] G. H. Golub and C. Van Loan, *Matrix Computations*, 4th ed. The Johns Hopkins University Press, 2013.
- [15] G. H. Golub, V. Klema, and G. W. Stewart, “Rank degeneracy and least squares problems,” Stanford University Department of Compute Science, Tech. Rep., 1976.
- [16] T. F. Chan and P. C. Hansen, “Some applications of the rank revealing QR factorization,” *SIAM Journal on Scientific and Statistical Computing*, vol. 13, no. 3, pp. 727–741, 1992.
- [17] —, “Low-rank revealing QR factorizations,” *Numerical Linear Algebra with Applications*, vol. 1, no. 1, pp. 33–44, 1994.
- [18] R. Vidal, Y. Ma, and S. S. Sastry, *Generalized Principal Component Analysis*. Springer, 2016.
- [19] F. Zhu, “Hyperspectral unmixing: Ground truth labeling, datasets, benchmark performances and survey,” *arXiv preprint arXiv:1708.05125*, 2017.
- [20] Y. Zhou, “A spatial compositional model for linear unmixing and endmember uncertainty estimation,” https://github.com/zhouyuanzxcv/Hyperspectral/blob/master/data/PaviaUniversity_corrected.mat, accessed may 2020.